Research Report

No. 83-1

STUDY OF THE RECEPTION
OF FREQUENCY DEHOPPED M-ARY FSK

FINAL REPORT FOR

THE DEPARTMENT OF COMMUNICATIONS
UNDER DSS CONTRACT NO. OSU82-00167

BY

P.H. WITTKE
P.J. MCLANE
P. MA

MARCH 1983

Queen's University at Kingston
Department of Electrical Engineering

STUDY OF THE RECEPTION OF FREQUENCY DEHOPPED M-ARY FSK

by

P.H. Wittke

P.J. McLane

P. Ma

Report No. 83-1

Final Report

Prepared for

The Department of Communications

Under DSS Contract No. OSU82-00167

Department of Electrical Engineering

Queen's University

Kingston, Ontario, Canada

March, 1983

ABSTRACT

A study of the reception of frequency dehopped noncoherent M-ary FSK is carried out. First, expressions for the signal spectrum are presented. Then the performance of a receiver consisting of a bank of energy detectors is studied. With the trend to hopped satellite systems at higher and higher frequency, and with ever increasing hopping rates, error in signal frequencies or frequency offsets may be present in the system, and in addition, instability or phase variation in the oscillators potentially may cause system performance degradation. Possible frequency offset and phase jitter are included in the theoretical development, in addition to the usual additive white Gaussian noise. Calculations of error performance degradation due to frequency offsets and thermal noise for both single user and multi-user environments, are presented. For multi-users, the circumstances under which windowed receivers provide improved error performance, are indicated. Detailed error rate calculations remain to be carried out for the phase noise theory that has been developed.

1. INTRODUCTION

Under the Space Sector military program, the Communications Research Centre has from the Department of National Defence the task of the development of spread spectrum modulation. The goal is to provide an electronic counter-countermeasures capability to military satellite communications. Recently, the trend in MIL-SATCOM has been to communications at EHF and the use of fast frequency-hopped, M-ary FSK spread spectrum signal structures. This report is on these signals and their reception.

In work under previous contracts with the Space Systems Section of the Department of Communications, encoding [1], and signal-shaping techniques [2], for phase-continuous FSK were developed which gave improved spectral occupancy and error performance. Also new, less complicated receiver structures were obtained [3-5]. However, as frequency hopping is carried out over large bands and at rates that are as high as possible, phase continuous modulation and coherent detection becomes beyond current technology.

Band occupancy remains an important issue from the point of view of minimizing the interference between adjacent users whose signalling power may differ dramatically. Thus, an expression for the spectrum of noncoherently frequency-hopped M-ary FSK is presented in section 2. Windowing in the receiver [6], which can be viewed as mismatching the receiver and signal, offers an increased rejection of adjacent channel interference at some

sacrifice in signal-to-noise performance. The optimum window remains an open question and there is the possibilty of signal shaping and coding not only to reduce adjacent channel effects but also to increase jam resistance. However it was felt that signal or receiver design must be carried out in the light of overall error performance, and so in section 3 of this research report we present an analysis of the basic energy detector used in noncoherent reception of M-ary FSK. The work is directed toward the evaluation of error performance in M-ary FSK where there is not only additive noise in the channel, but in addition there may be a frequency offset due to imperfections or inaccuracies in the hopping-dehopping. As well, there may be a phase jitter on the tones themselves. In the latter part of the report some computations on the error rate for multi-user M-ary FSK environments are presented.

2. THE SPECTRUM OF NONCOHERENTLY HOPPED M-ARY FSK

In this section of the report we will derive an expression for the spectrum of noncoherently hopped M-ary FSK. As expected, the spectrum appears as a superposition of the spectra of the individual component pulses each centred at the M possible frequencies.

The modulated signal of interest is of the form

$$s(t) = \sum_{n=-\infty}^{\infty} g(t-nT)\, h(a_n, t-nT),$$

where $g(t)$ is any amplitude shaping of the pulse that may have

occurred and the angle of the pulse is given by

$$h(a_n,t-nT) = \cos[\omega_c t + a_n \Delta\omega(t-nT) + p(t-nT) + \theta_n]$$

For M-ary transmission a_n can take on the values $\pm1,\pm3,..\pm(M-1)$, which correspond to the frequencies $\omega_c+(2i-1)\Delta\omega$, $i=\pm1,..\pm M/2$. Any shaping of the instantaneous frequency is described by $p(t)$ and the incoherent hopping results in statistically independent random initial phases θ_n, that are assumed to be uniformly distributed over $(0,2\pi)$.

The signal can be written in terms of a complex baseband equivalent

$$s(t) = \mathrm{Re}\{\rho(t)\exp[j\omega_c t]\}$$

where

$$\rho(t) = \sum_{n=-\infty}^{\infty} g(t-nT)\exp\{j[a_n \Delta\omega(t-nT) + p(t-nT) + \theta_n]\},$$

Here Re denotes the real part, and * as a superscript denotes the complex conjugate.

The autocorrelation function will be used to find the signal spectrum. There follows

$$R(t,t+\tau) = (1/4)[E\{\rho(t)\rho(t+\tau)\}\exp j\omega_c(2t+\tau) + E\{\rho(t)\rho^*(t+\tau)\}\exp -j\omega_c\tau + E\{\rho^*(t)\rho(t+\tau)\}\exp j\omega_c\tau + E\{\rho^*(t)\rho^*(t+\tau)\}\exp -j\omega_c(2t+\tau)].$$

Due to the assumption of uniformly distributed θ_n, $E\{\rho(t)\rho(t+\tau)\}=0$, and the first and last terms in the expression for $R(t,t+\tau)$ vanish. Thus,

$$E\{\rho(t)\rho^*(t+\tau)\} = \sum_{n=-\infty,m=-\infty}^{\infty} g(t-nT)g(t+\tau-mT)\ \xi$$

where

$$\xi = E\{\exp j[a_n \Delta\omega(t-nT) - a_m \Delta\omega(t+\tau-mT) + p(t-nT) - p(t+\tau-mT) + \theta_n - \theta_m]\}$$

$$= E\{\exp -ja_n \Delta\omega\tau\}.\exp -j[p(t+\tau-nT) - p(t-nT)].\delta_{m,n}$$

Now

$$E\{\exp -ja_n \Delta\omega\tau\} = (2/M) \sum_{i=1}^{M/2} \cos(2i-1)\Delta\omega\tau \ ,$$

and finally,

$$E\{\rho(t)\rho^*(t+\tau)\} = \sum_{n=-\infty}^{\infty} g(t+\tau-nT)g(t-nT).(2/M)\sum_{i=1}^{M/2} \cos(2i-1)\Delta\omega\tau.$$

$$.\exp -j[p(t+\tau-nT) - p(t-nT)]$$

The autocorrelation function

$$R(t,t+\tau) = (1/2)\mathrm{Re}\{E\{\rho(t)\rho^*(t+\tau)\}\exp -j\omega_c\tau\}$$

is a function of t. In other words the signal s(t) is not wide-sense stationary but is in fact cyclostationary (see [14]), that is, $R(t+T,t+\tau+T) = R(t,t+\tau)$. This can be dealt with as follows. Since in practice we do not have a precise time origin, we can assume that the origin is uniformly distributed over (0,T)

$$f_t(\eta) = (1/T) \qquad 0 \leq \eta \leq T$$

$$= 0 \qquad \text{elsewhere.}$$

The average autocorrelation function is

$$R(\tau) = E_t\{R(t,t+\tau)\}.$$

After simplification this reduces to

$$R(\tau) = (2MT)^{-1} \sum_{i=1}^{M/2} \cos[(2i-1)\Delta\omega\tau].[\exp[-j\omega_c\tau]\{z(\tau)*z^*(-\tau)\} +$$

$$+ \exp[j\omega_c\tau]\{z^*(\tau)*z(-\tau)\}],$$

where * denotes the convolution, and $z(t) = g(t)\exp -jp(t)$. The autocorrelation consists of the sum of two terms. One corresponding to the spectrum centred at ω_c, and the other the mirror

image at $-\omega_c$. The part about ω_c is given by

$$S(\omega) = (4MT)^{-1} \sum_{\substack{i=-M/2 \\ i\neq 0}}^{M/2} S_z(\omega_c-(2i-1)\Delta\omega)$$

where

$$S_z(\omega) = FT\{z(\tau)*z^*(-\tau)\} = |Z(\omega)|^2,$$

$$Z(\omega) = FT\{z(\tau)\}$$

and

FT{z} denotes the Fourier transform of z.

3 ERROR PERFORMANCE OF NONCOHERENT M-ARY FSK IN THE PRESENCE OF FREQUENCY OFFSET, PHASE JITTER AND ADDITIVE NOISE

In the system under consideration, ideally one of M frequencies f_i, i=1,2,..M, with orthogonal frequency spacing is transmitted in the time interval (-T/2,T/2). Due to imperfections in the transmission system the detected tone is not at the precise frequency f_i, but there is a frequency offset or error of Δf Hz. Also, the phase of the sinusoid available for processing has a random component $\phi(t)$, which varies over the observation interval, and it is assumed that there is additive noise in the channel. Thus the received signal is given by

$$s_i(t)=A\cos(\omega_i t + \Delta\omega t + \phi(t) + \phi_0) + n(t), \quad i=1,2,...M$$

The detection will be carried out by noncoherent energy detectors and so without restriction we can for convenience take $\phi_0=0$.

The receiver consists of M energy detectors of the form shown in Figs.1 and 2 and the decision is made that the frequency

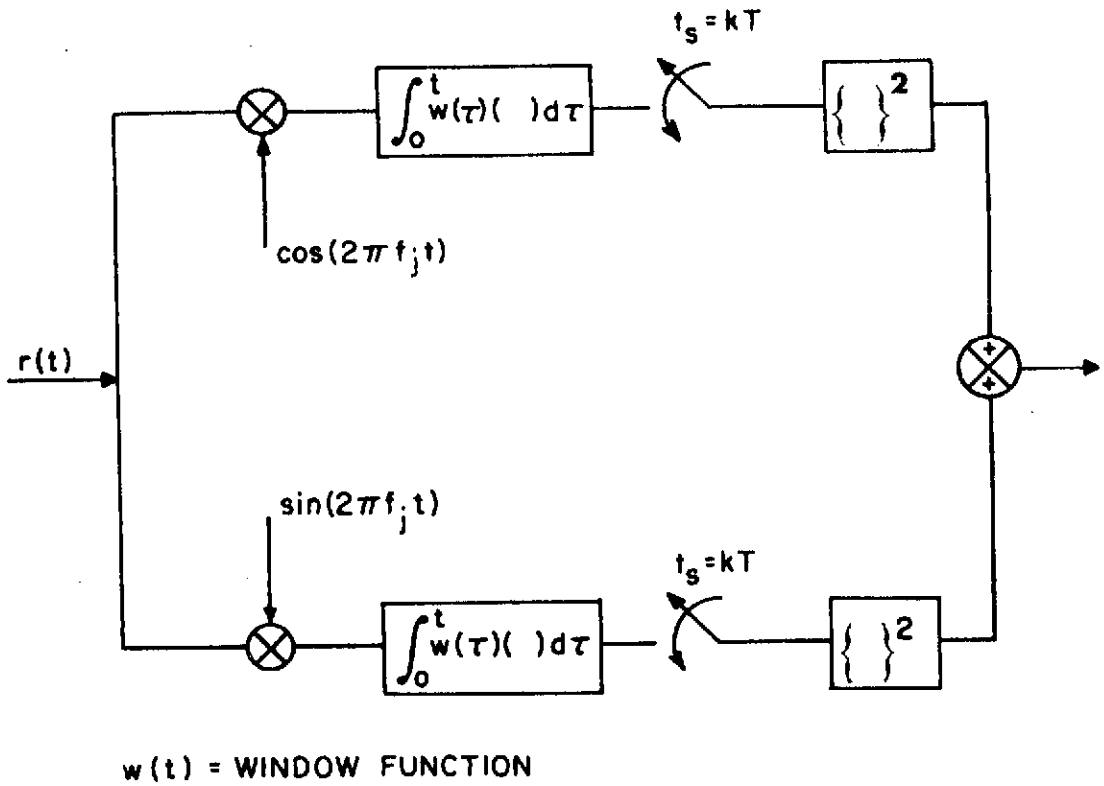

Fig. 1: An energy detector with a weighted integrator for incoherent, FSK detection.

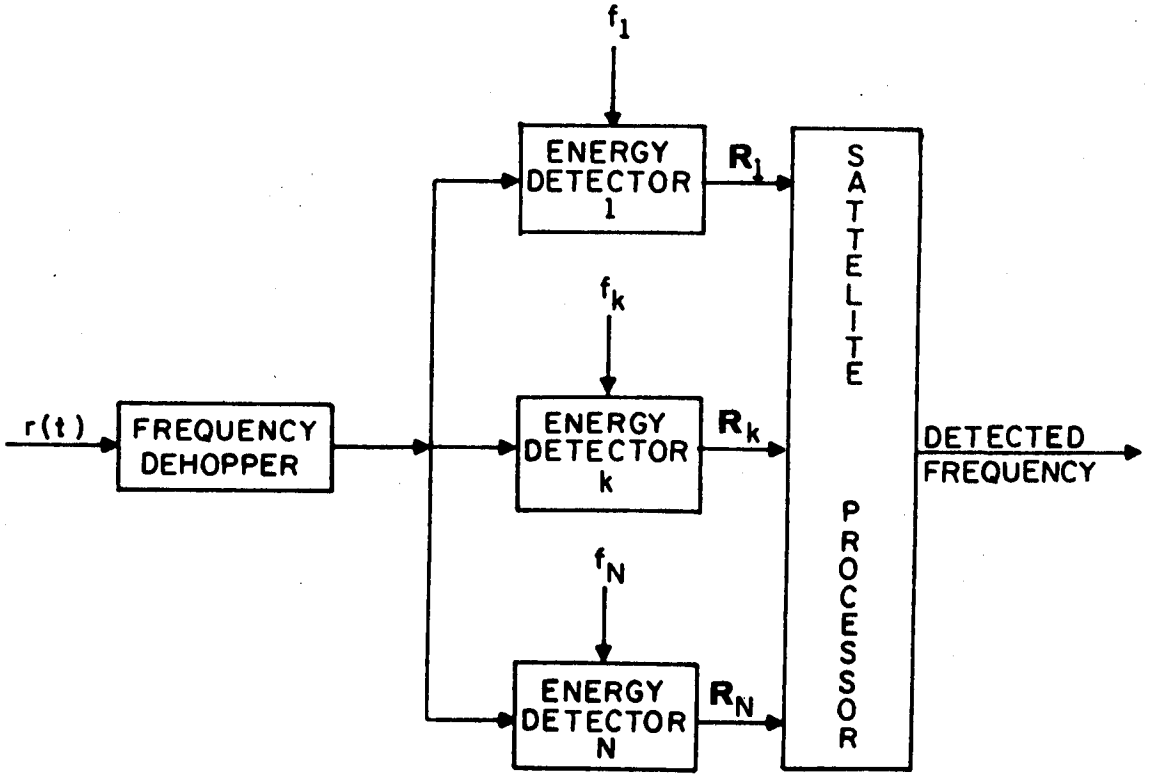

Fig. 2: A bank of energy detectors for multi-user, MFSK detection. The input signal to the receiver is first dehopped using code used for group frequency hopping in the transmitter.

corresponding to that of the detector with the largest output, was in fact sent. We will deal with the probability of error given s_1 sent, which from the symmetry of the problem is the overall probability of error. Suppose the magnitude of the output of the i^{th} detector is R_i, $i=1,2,\ldots M$. An error occurs when $R_i > R_1$, for some $i=2,3,\ldots M$. Thus the probability of error is given by

$$P_e = 1 - {}_0\int^{\infty} dR_1 \; {}_0\int^{R_1} \cdots {}_0\int^{R_1} f(R_1, R_2, \ldots R_M) dR_2, \ldots dR_M$$

For convenience we can write the output of the i^{th} detector in complex notation $z_i = x_i + jy_i$. Then $R_i = |z_i|$,

$$z_1 = \frac{A}{2} \int \exp\{j(\Delta\omega t + \phi(t))\} dt + \int n(t) e^{-j\omega_1 t} \, dt$$

Note, where the limits of integration are not indicated explicity, they are $(-T/2, T/2)$.

If the phase noise $\phi(t)$ is fairly small over $(-T/2, T/2)$, the first term in the expression for z_1 is well-approximated by

$$\frac{A}{2} \int e^{j\Delta\omega t}(1 + j\phi(t)) dt =$$

$$(A/2)[T(e^{j\Delta\omega T/2} - e^{-j\Delta\omega T/2})/j\Delta\omega T + j\int \phi(t) e^{j\Delta\omega t} dt]$$

Thus

$$z_1 = (AT/2)[\text{sinc}(\Delta\omega T/2) + jT^{-1} \int \phi(t) e^{j\Delta\omega t} dt] + \int n(t) e^{-j\Delta\omega_1 t} \, dt$$

The common notation sinc $x = \sin x/x$ has been used.

The inaccuracy in the above approximation appears very small

for usual levels of phase noise. For example for a jitter of 30^{o}, which for most reasonable oscillators would be considered a large jitter, the error in the linear approximation is 2.4 %.

For orthogonal signalling $(\omega_i - \omega_1)T/2 = k\pi, \quad k=\pm1,\pm2,..$

Thus $$z_i = (A/2)\int \exp\{j[\omega_1+\Delta\omega-\omega_i)t + \phi(t)]\}dt + \int n(t)\exp\{-j\omega_i t\}\, dt$$

$$= (A/2)\int \exp\{j[(\Delta\omega-2k\pi/T)t + \phi(t)]\}dt + \int n(t)\exp\{-j\omega_i t\}dt$$

Again we will make the assumption that $\phi(t)$ is not too large over $(-T/2,T/2)$ and approximate $\exp[j\phi(t)]$ by $1+j\phi(t)$. After some simplification we obtain

$$z_i = C_i P + j(A/2)\int \phi(t)\exp\{j[\Delta\omega-2k\pi/T]t\}dt + \int n(t)\exp\{-j\omega_i t\}dt$$

$$i=2,3,..M$$

$$z_1 = P + j(A/2)\int \phi(t)\, \exp\{j\Delta\omega t\}dt + \int n(t)\exp\{-j\omega_1 t\}dt$$

where $P = (AT/2)\mathrm{sinc}(\Delta\omega T/2)$ and $C_i = (-1)^{k+1}/(1-2k\pi/(\Delta\omega T))$, and k is the integer corresponding to the particular orthogonal spacing of f_i.

If we assume that $\phi(t)$ and $n(t)$ are Gaussian processes, then the random variables x_i and y_i are Gaussian. It is usual to assume that the additive noise is Gaussian. Also the assumption of Gaussian phase noise is common. It can be shown [7], that for a first order phase-locked loop the phase is asymptotically

Gaussian and well-approximated by the Gaussian distribution even at quite moderate signal-to-noise ratios. As well, in another application, one of the authors measured phase noise to be Gaussian with a high degree of accuracy.

The means of the Gaussian variables are

$$E\{z_1\}=E\{x_1\}=P, \qquad E\{z_i\}=E\{x_i\}=C_k P \quad \text{for } i\neq 1$$

$$E\{y_i\}=0$$

We have derived expressions for the various joint moments $E\{x_i y_j\}$ under the assumption that the additive noise is white. Unfortunatley in the most general case there is correlation between all the components and the analysis does not simplify.

3.1 General Method of Analysis

To find the distribution of the envelopes $R_1, R_2, \ldots R_M$, we will use the technique originally used by Rice [8], to obtain envelope distributions for Gaussian noise. Let us write our observed variables as a Gaussian vector

$$X = [x_1, y_1, x_2, y_2, \ldots . x_M, y_M]$$

with mean

$$M_X = [P, 0, C_2 P, 0, \ldots . C_M P, 0]$$

and covariance matrix ρ with general element ρ_{ij}. Let λ with elements λ_{ij} be the inverse of ρ and let $|\rho|$ denote the determinant of ρ. Then since X is gaussian, its density function is given by

$$f(x_1, y_1, x_2, \ldots y_M) = (2\pi)^{-M} |\rho|^{-1/2} \exp\{-1/2 (X-M_X)\lambda (X-M_X)^t\}$$

Here t denotes the matrix transpose.

The joint distribution of $R_1, R_2, \ldots R_M$ is obtained in two

steps. First carry out the change of variables

$$x_i = R_i \cos\theta_i$$

$$y_i = R_i \sin\theta_i, \qquad i=1,..M,$$

for which the Jacobian of the transformation is $R_1 R_2 \ldots R_M$. Thus $f(R_1,\theta_1,R_2,\ldots .R_M,\theta_M)=f_X(x_1\cos\theta_1,\ldots x_M\sin\theta_M).R_1..R_M$. The density function of $R_1,R_2,.. ..R_M$ is obtained by integrating over the extraneous θ variables. This may be difficult or at least messy in practice. In particular cases this has been possible using modified Bessel function generating functions

$$\exp\{z\cos\theta\}=I_o(z) + \sum_{k=1}^{\infty} I_k(z)\cos(k\theta)$$

$$\exp\{z\sin\theta\}=I_o(z) + 2\sum_{k=0}^{\infty} (-1)^k I_{2k+1}(z)\sin[(2k+1)\theta]$$

$$+ 2\sum_{k=1}^{\infty} (-1)^k I_{2k}(z)\cos(2k\theta)$$

This procedure yields a density function in terms of series of Bessel functions. An example will be given in the next section of this report.

3.2 Distribution of the Output of an Individual Energy Detector

As a first fairly simple case let us find the probability density function of the sampled output of an individual energy detector. The density function of the components is

$$f(x_1,y_1)=(2\pi)^{-1}|\rho|^{-1/2}\exp\xi$$

where the exponent $\xi = (-1/2)[\lambda_{11}(x_1-P)^2+\lambda_{22}y_1^2 + 2\lambda_{12}(x_1-P)y_1]$.

Here

$$|\rho| = (\rho_{11}\rho_{22}-\rho_{12}^2)$$

and

$$\lambda = \frac{1}{|\rho|}\begin{vmatrix}\rho_{22} & -\rho_{12}\\ -\rho_{12} & \rho_{11}\end{vmatrix}$$

After the change of variables $x_1=R\cos\theta$, $y_1=R\sin\theta$, and simplification we obtain for the exponent

$$\xi = (-1/2)[\lambda_{11}P^2 + (\lambda_{11}+\lambda_{22})R^2/2 + (R^2/2)\{(\lambda_{11}+\lambda_{22})^2+4\lambda_{12}^2\}^{1/2}\cdot$$
$$\cdot\cos(2\theta-2\phi) - 2PR(\lambda_{11}^2+\lambda_{12}^2)^{1/2}\cos(\theta-\psi)]$$

where

$$\phi = (1/2)\tan^{-1}[2\lambda_{12}/(\lambda_{11}-\lambda_{12})], \text{ and } \psi = \tan^{-1}[\lambda_{12}/\lambda_{11}].$$

If we make the change of variable $\theta_1=\theta-\phi$ and as suggested above use the Bessel function expansion

$$\exp\{z\cos\theta_1\} = I_o(z) + 2\sum_{k=1}^{\infty} I_k(z)\cos k\theta_1$$

we obtain the expression for the density function of the detector output

$$f(R) = R(\rho_{11}\rho_{22}-\rho_{12}^2)^{-1/2}\exp\{(-1/2)[\lambda_{11}P^2+(\lambda_{11}+\lambda_{22})R^2/2]\cdot$$
$$\cdot[I_o(k_1)I_o(k_2) + 2\cos(\psi-\phi)\sum_{k=1}^{\infty} I_k(k_1)I_{2k}(k_2)]$$

where

$$k_1 = (-R^2/4|\rho|)[(\rho_{22}-\rho_{11})^2+\rho_{12}^2]^{1/2},$$

and

$$k_2 = (RP/|\rho|)[\rho_{22}^2 + \rho_{11}^2]^{1/2}.$$

3.3 Binary FSK with Frequency Error

Let us consider the error performance of a noncoherent detection system for binary FSK, when there is frequency error and additive channel noise, but no phase jitter. This is the easiest of the cases currently under consideration. Then

$$x_1 = \int n(t)\cos\omega_1 t\, dt + P$$

$$y_1 = -\int n(t)\sin\omega_1 t\, dt$$

$$x_2 = k_2 P + \int n(t)\cos\omega_2 t\, dt$$

$$y_2 = -\int n(t)\sin\omega_2 t\, dt$$

$$E\{z_1\} = E\{x_1\} = P$$

$$E\{z_2\} = E\{x_2\} = C_2 P$$

We will assume that the additive noise is white with two-sided spectral density $N_0/2$ watts/Hz. Then

$$\rho_{11} = \rho_{22} = \rho_{33} = \rho_{44} = N_0 T/4$$

$$\rho_{ij} = 0 \text{ for } i \neq j.$$

The procedure outlined above carries out easily. In effect R_1 and R_2 are independent Rician random variables [8] with density function

$$f(R_i) = (R_i/\sigma_i^2)\exp\{-(a_i^2 + R_i^2)/2\sigma_i^2\}\, I_0(a_i R_i/\sigma_i^2)$$

Here $a_1 = P$, $a_2 = k_2 P$, and $\sigma_1^2 = \sigma_2^2 = N_0 T/4$

The probability that one Rician variable exceeds another independent Rician variable can be expressed in terms of Marcum's

Q function [9,p.587]. Thus the probability of error is given by

$$p_e = Q(\sqrt{a},\sqrt{b}) - [\nu^2/(1+\nu^2)] \exp\{-(a+b)/2\}\ I_o(\sqrt{ab}) \qquad (1)$$

where the Marcum's Q function is given by

$$Q(a,b) = {}_b\int^{\infty} \exp\{-(a^2+x^2)/2\}\ I_o(ax)\ x\ dx$$

$$a = 2C_2^2P^2/N_0T, \qquad b = 2P^2/N_0T$$

$$\nu = 1.$$

Setting $C_2 = 0$, should yield the previously known result for the noncoherent detection of binary FSK

$$P_e = Q(0,\sqrt{b}) - (1/2)\exp\{-b/2\}$$

$$= (1/2)\exp\{-P^2/N_0T\}.$$

The last step follows since $Q(0,\sqrt{b}) = \exp\{-b/2\}$ and $I_o(0) = 1$.

We wish to use McGee's recursive method for computing Marcum's Q-function [10]. Accordingly, we may apply the tranformation in (A-3-1), p.586, of [9] to write (1) in the form

$$P_e = 1 - Q(\sqrt{b},\sqrt{a}) + (1/2)\exp\ [-(a+b)/2]\ I_o\ (\sqrt{ab}) \qquad (2)$$

McGee's algorithm computes $1 - Q(\sqrt{b},\sqrt{a})$ using a simple recursive procedure.

We have used the formula in (2) to compute estimates to P_e in the following two cases:

(i) The symbol error probability for M-ary FSK modulation in a single user environment with frequency errors in the input signal.

(ii) The symbol error probability for binary FSK modulation in a multi-user environment with frequency errors in the input, multi-user tones.

Our ultimate goal is to obtain good estimates of P_e for up to M = 8 for a multi-user environment with frequency errors in the input tones. We can also handle frequency errors in the correlator sinusoids using Stein's general formula (equation (8-2-12) of [9]). However, the computations are left for further study.

3.4 M-ary FSK with no Frequency Error

First, we consider M-ary FSK modulation when the transmitted signals are orthogonal and are identical in format to the signals used in the energy detectors in the receiver. Then, as shown in problem 7.9 of [11], the symbol error probability is given by

$$P_e = \sum_{k=1}^{M-1} (-1)^{k+1}/(k+1) \binom{M-1}{k} \exp[-kE/(k+1)N_o] \qquad (3)$$

where E is the signal energy,

$$\binom{n}{k} = \frac{n!}{k!(n-k)!}$$

and No/2 is the spectral height of the white Gaussian noise which is the only assumed form of disturbance in the present case. An upper bound to P_e can easily be obtained by using the union bound. This bound on P_e is

$$P_e < [(M-1)/2] \exp[-E/2N_o] \qquad (4)$$

and the bound is the exact error probability when M=2.

In Fig. 3 we plot P_e versus E/N_o for various M. Note that performance degrades gracefully for increasing M. In fact, if the abscissae was replaced by the energy per bit-to-noise ratio

$$E_b/N_o = E/N_o \log_2 M$$

performance would get better for increasing M. However, this is at the expense of an increase in required channel bandwidth as the minimal tone separation is 1/T Hz for signal orthogonality.

In Fig.4 we compare P_e in (3) with its upper bound in (4) for various M. The upper bound is quite close to the error probability in terms of the spread in E/N_o. We will also find that the union bound gives quite accurate results even in the presence of frequency errors in the input tones to the energy detectors. However, in this case, exact results appear difficult to get. Instead we use a lower bound to go along with the upper bound based on the union bound.

3.5 M-ary FSK with Frequency Error: Single User Case

Our expression above for the system error probability depends strongly on the following two facts:

(i) The only energy detector output with a non-zero mean value is the one corresponding to the input frequency of the signal component of the received waveform

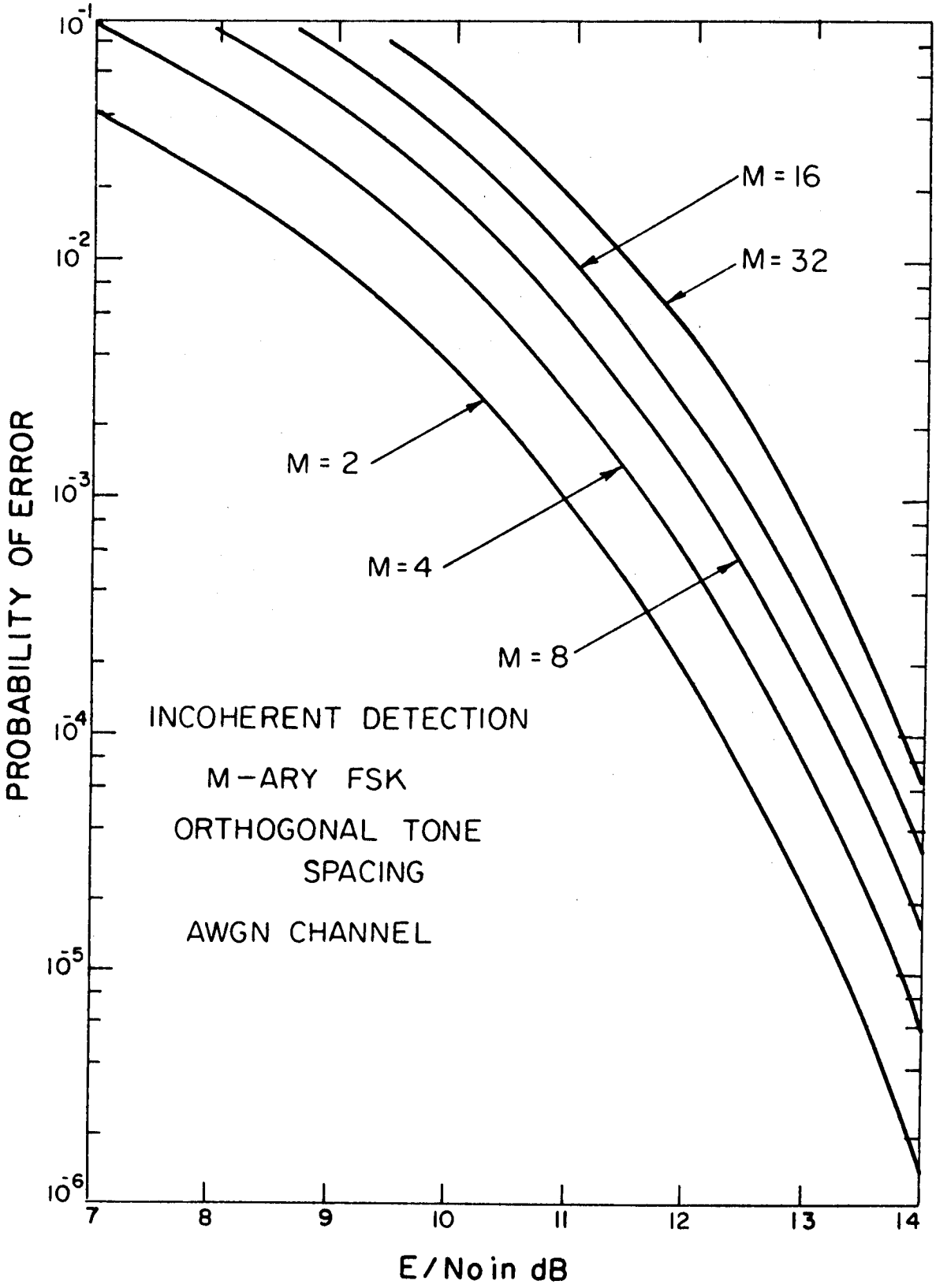

Fig. 3: Error performance of M-Ary FSK for an AWGN channel.

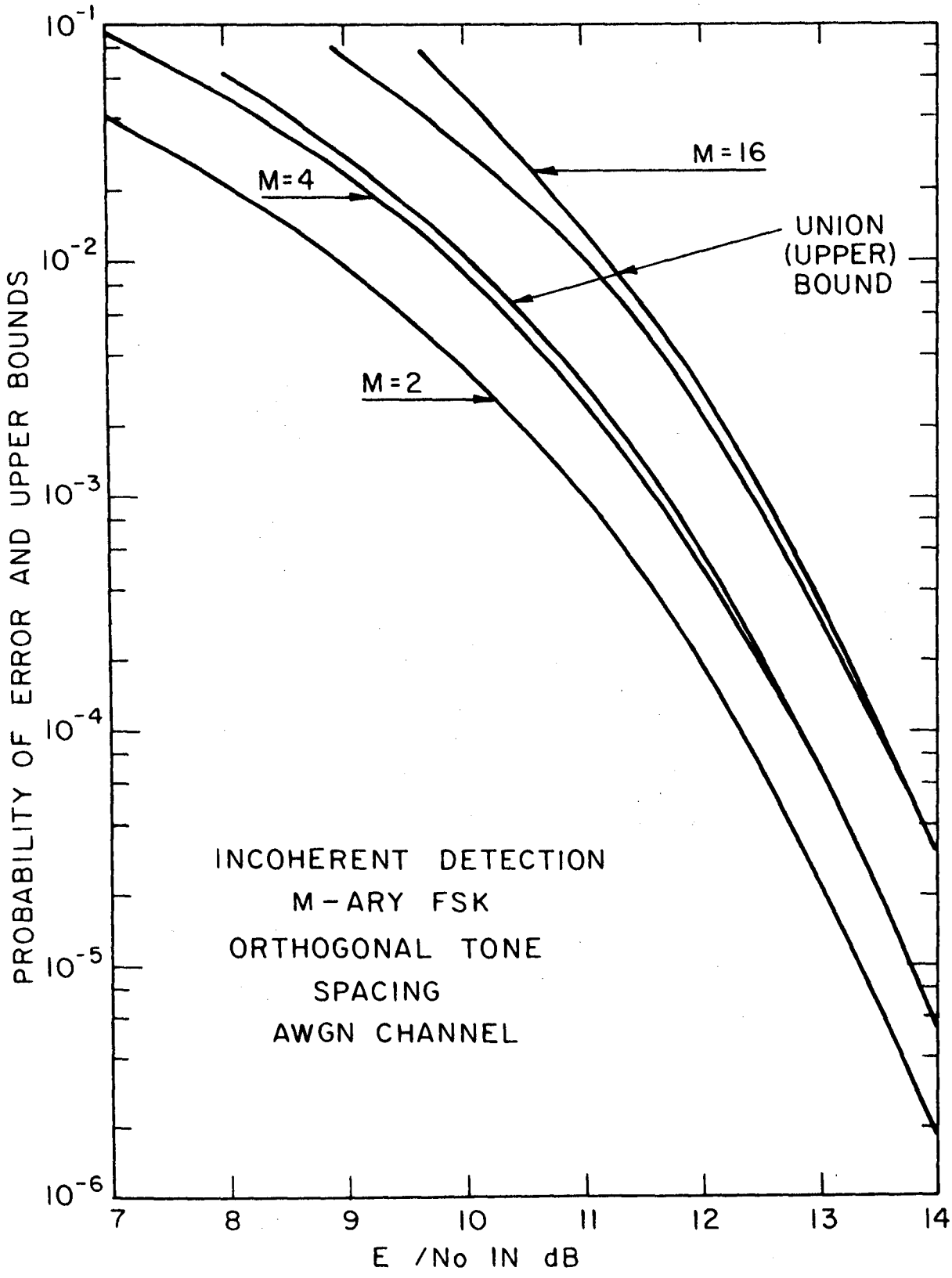

Fig. 4: Error performance and its upper bound based on the union bound for an AWGN channel.

and

(ii) the noise outputs of all energy detectors are independent.

In the analysis to follow we assume that the correlation waveforms in the energy detector are orthogonal. That is, unlike the input waveforms, they are not subjected to frequency errors. Thus the item noted as (ii) above carries over into our analysis. However, as just mentioned, we allow the tone inputs to the receiver to undergo frequency errors. This gives a non-zero mean value to each energy detector and leads to much complication in the error analysis.

Let us first consider the case of binary FSK with a common frequency error in both tones of Δf Hz. We introduce a change in mathematical detail which does not alter the final results, in particular, the calculations were carried out with the integrators in Fig. 1 operating over [0,T] rather than [-T/2, T/2]. Then the formula for a and b in (1) is

$$\begin{aligned} b &= \frac{E}{N_o} \left(\text{sinc}^2 2\pi\Delta fT + \text{cinc}^2 2\pi\Delta fT\right) \\ a &= \frac{E}{N_o} \left[\text{sinc}^2 2\pi(\Delta fT+m) + \text{cinc}^2 2\pi(\Delta fT+m)\right] \end{aligned} \tag{5}$$

where sinc x = $\sin x/x$, cinc $x = (1-\cos x)/x$ and m is the spacing between mark and space tones in multiples of T^{-1}.

For given ΔfT and m we can now evaluate the formula in (2) for a range of E/N_o. Our computational results are given in Fig. 5 for $m = 1$ and the worst case $\varepsilon = \Delta fT$. A frequency error of 10%

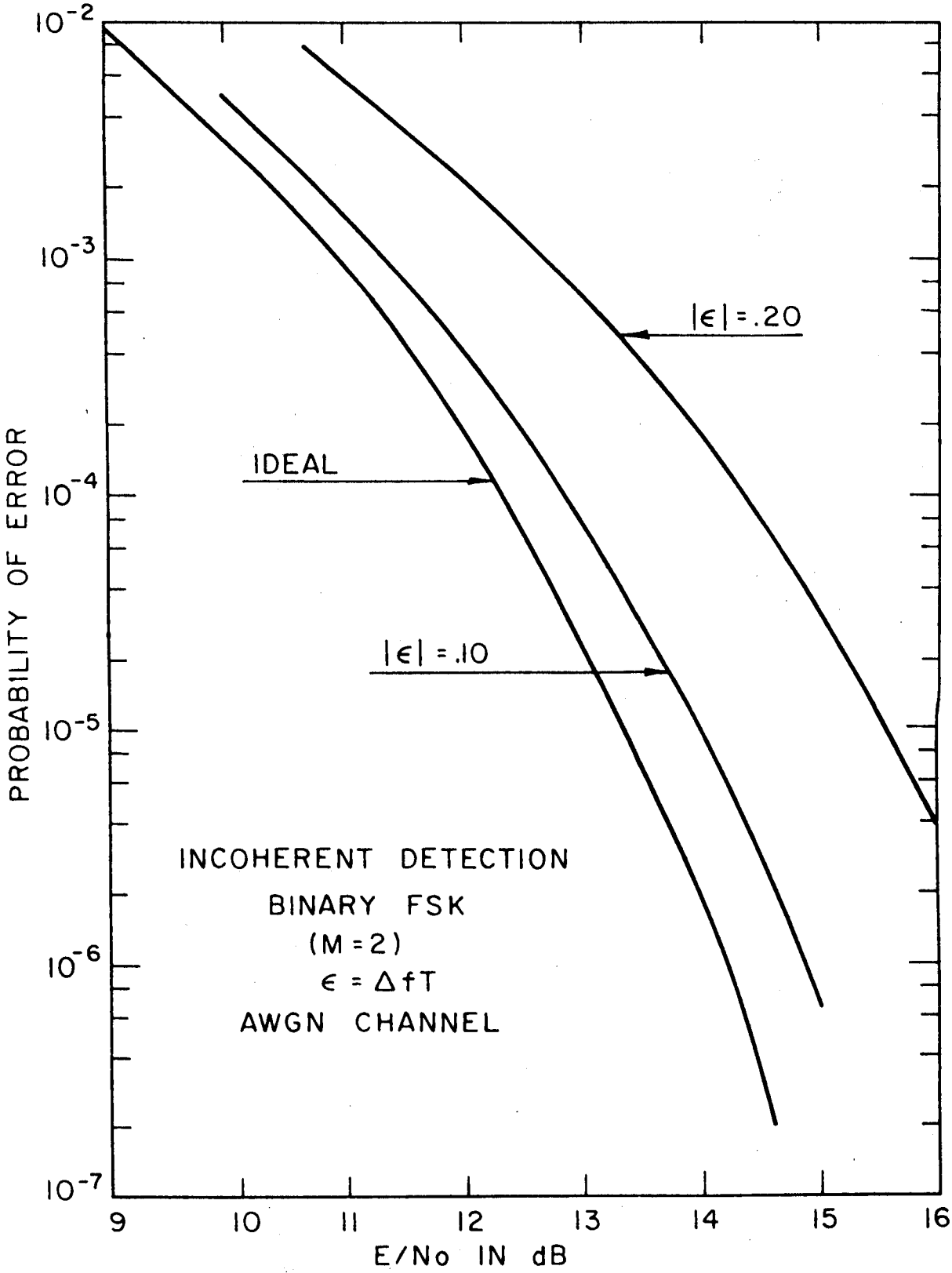

Fig. 5: Error performance of Binary FSK with frequency errors in the modulation tones for an AWGN channel.

of the baud interval results in a loss in E/N_o of .3 dB while a 20% error gives a loss of 2dB at practical error rates. Clearly the maximum, tolerable frequency error is between 10% and 20% of the reciprocal of the baud interval, T^{-1}.

We now consider the case of M = 4, again with a common frequency error in the input tones. We will use error bounds to estimate P_e in this case as a computable formula appears difficult to get. First consider an upper bound based on the union bound. From a computation with equations (2) and (5) above it is seen that P_e for the binary case is a function of m and Δf where m is a multiple of 1/T. For quaternary modulation, worst case results are obtained when P_e is computed for either tone 2 or 3 (the intermediate tones) in the set of 4 modulation tones. The union bound is obtained by computing the error probability for all pairwise tone detections. Thus for the worst case

$$P_e < 2\, P_e\,(\Delta f,1) + P_e\,(\Delta f,2) \qquad (6)$$

where $P_e(\Delta f,m)$ is computed from (2) and (5). Our upper bounds are shown in Fig. 6 for a range of E/N_o.

Our lower bound is quite simple and is based on a method Forney used to bound the performance of maximum likelihood sequence receivers [12]. Suppose we ask the receiver for Quaternary FSK to distinguish only between any two tones. It does so with $P_e = P_e(\Delta f,m)$. At best, the performance of the Quaternary FSK receiver can be no better than $P_e(\Delta f,1)$. Thus $P_e > P_e\,(\Delta f,1)$ and this lower bound is shown in Fig. 6. The spread in the bounds is

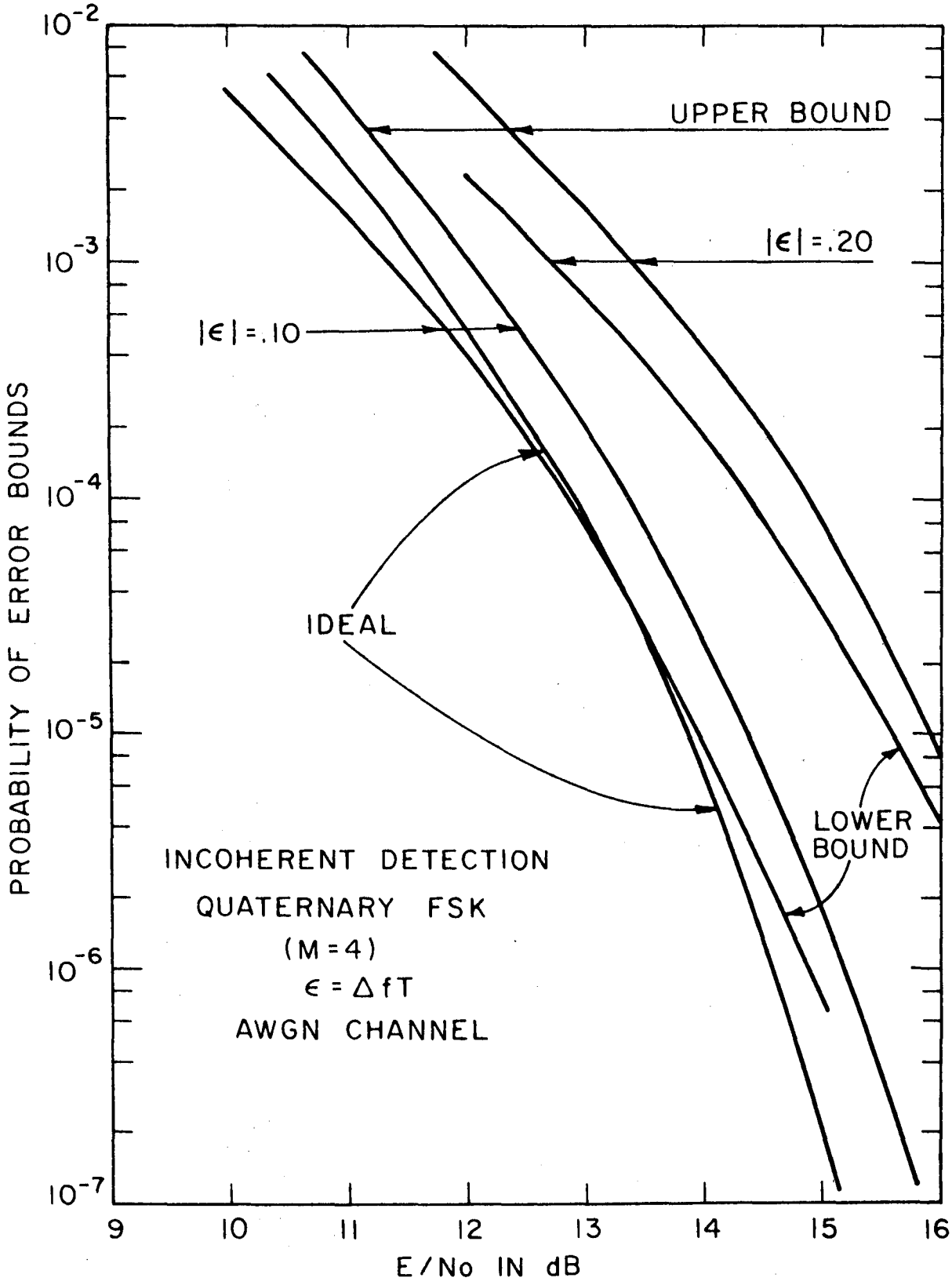

Fig. 6: Upper and lower bounds to the error probability for Quaternary FSK with frequency errors and an AWGN channel.

less than .5dB in E/N_o. To get our estimate of P_e draw a line midway between the bounds. This estimate is accurate to 0.25dB in E/N_o.

In Fig. 7 we present our upper and lower bounds for the Octonary (M=8) FSK case. Again the bounds are quite tight on the basis of a spread in E/N_o in dB. The upper bound here is

$$P_e \leq 2\,P_e(\Delta f,1) + 2\,P_e(\Delta f,2) + 2\,P_e(\Delta f,3) + P_e(\Delta f,4) \qquad (7)$$

Note that Quaternary and Octonary FSK are less sensitive to orthogonality perturbation than binary FSK. This is because the primary source of interference comes from adjacent tones. The interference is thus most critical in a binary FSK system where decisions must always be made relative to an adjacent tone frequency. This fact has aided our bounding procedure of P_e. We have used the lower bound to be an exact result from the binary FSK case. It is usually quite close in E/N_o to the upper bound based on the union bound for M=4 and M=8.

3.6 Binary FSK with Frequency Error: Multi-User Case

Let the number of potential users of a FDMA/BFSK system be N. There are 2 assigned frequencies per user and thus L = 2N potential frequencies for detection. Thus the receiver represented in Figs. 1 and 2 is a bank of L energy detectors. However as pointed out in [13], these detectors likely would be realized using a single Fourier transform.

Let K of the N users be "on the air". The performance of the

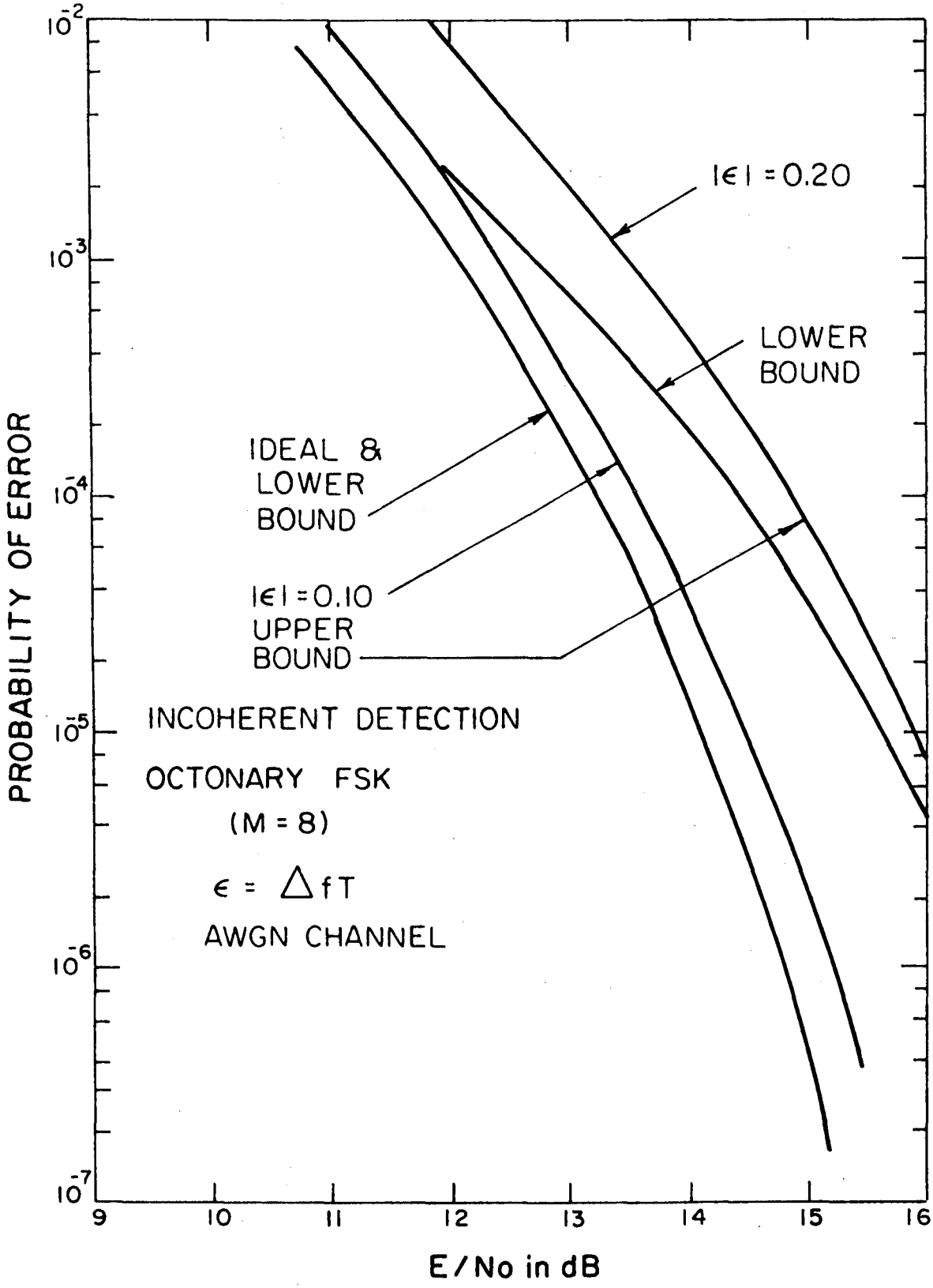

Fig. 7: Upper and lower bounds to the error probability for Octonary FSK with frequency errors and a AWGN channel.

system could be determined by assigning K-1 interfering frequencies to N-2 frequency slots and assigning each tone a random phase and frequency error. The a and b parameters for Stein's formula could then be found and these would depend on the K-1 random phases and frequency errors. The error probability would be determined using Monte Carlo techniques which would average the error probability over each tone setting, tone random phase and tone frequency error.

We are primarily interested in receivers with weighted integrators: the so-called windowed receiver. The a and b parameters are hard to determine for many popular window functions. Accordingly we decided to evaluate the a and b parameters for Stein's formula using the FFT algorithm. Again the K-1 out of N-2 frequency slots were chosen with the two tones for detection placed at mid-frequency band. This will give the worst-case interference and hence worst-case error probability. If we use an FFT algorithm which calculates all harmonics and if the tone spacing between user frequencies is $2T^{-1}$, the number of FFT frequencies will be 8N. This $2T^{-1}$ tone spacing is required due to the loss in frequency resolution in windowed receivers. That is, if an input tone has frequency k/T, significant energy in the windowed receiver appears at tone frequencies adjacent to the input frequency. Thus, a windowed receiver requires double the bandwidth of a system with a standard, rectangular window. However, with frequency error the rectangular window may not have high enough rejection of adjacent tones. Thus, tone spacing must

be increased and this leads to a greater system bandwidth than for the windowed receiver [6].

For the mark tone which we assume is the tone to be detected, we have

$$b = \frac{\lambda E}{N_o} \mid \nu_m \mid^2 \tag{7a}$$

and for the space tone

$$a = \frac{\lambda E}{N_o} \mid \nu_s \mid^2 \tag{7b}$$

Now a and b, through the FFT outputs ν_m and ν_s, depend on the frequency assignment, the random phases and the random frequency errors for the K-1 interferers.

The parameter λ is given by

$$\lambda = \frac{\left(\sum_{i=1}^{N^1} w_i\right)^2}{N^1 \sum_{i=1}^{N^1} w_i^2} \tag{8}$$

where N^1 is smallest power of 2 greater than or equal to 8N, w_i are the window samples and $10\log_{10} \lambda^{-1}$ represents the loss in signal-to-thermal noise ratio due to the receiver window function. In our input to the FFT the tones are complex exponential functions so as to model an in-phase and quadrature processor.

For a fixed frequency assignment and set of random phases and frequency errors, the error probability is given by (2) and (7). The average error probability is found by averaging over all

frequency assignments, random phases and random frequency errors using Monte Carlo methods. In our model, interfering tones are allowed to be more powerful than the data tones of the user. In one case these tones were 0dB, 3dB and 10dB higher than the data tone on an equally probable basis. The advantage of a windowed receiver in this case, was found to be clear. The results were obtained by averaging over many sets of frequency errors, random phases and random amplitudes for the interfering tones.

A typical set of calculations for our model are presented in Figs. 8 and 9. For the data in Fig. 8 we have 25 potential users each with a uniform random frequency error over $[-.2/T, .2/T]$. For Fig. 8 all users are assumed to be at equal power levels. The parameter used to set the Kaiser window function [6] was $\beta=1.8\pi$ and from (8) it follows that the loss in signal-to-thermal noise ratio is 1.6dB. We see from Fig. 8 that due to this loss the windowed receiver gives a very marginal improvement in performance only at very low error rates and thus the window is not required for the equal power case. In all our calculations data tones have been taken to be at adjacent frequencies. The σ marked on our curves is the maximum standard deviation of the sample error probability relative to the average result that is plotted.

In the calculations for Fig. 9 we have not placed all the interference at the same power levels as the data tone to be detected. In the worst case the interference is either equal, 3dB higher or 10dB higher than the data tone and all occur with equal

probability. Here, as we see from Figure 9, the window is essential for acceptable error probability. In the other case considered, the 3dB and 10dB interferences each occur with probability 1/8 whereas the 0dB interference level occurs otherwise. Again the window is needed to achieve reasonable error rates, even if the system is lightly loaded.

This performance is expected as the window produces low sidelobes which attenuate interfering, non-orthogonal, tones, but at the cost of a loss in signal-to-thermal noise ratio. For the window to be effective the loss in signal-to-thermal noise due to multi-user interference must be greater than the loss due to the window. In all cases our computed results have been average over 300 random samples of frequency assignment, random phase and frequency error. To compute one point on our error probability curves took approximately .5 hours of CPU time on a VAX 11/750. Most of the time is spent in computing FFT's and this will be speeded up considerably with the installation of our array processor.

4. Conclusions

The performance of a Binary FSK receiver can be analyzed in the presence of phase noise, frequency errors and thermal noise. Calculations in the general case remain to be carried out.

The performance of MFSK for single user environments and frequency errors can be effectively estimated with upper and lower

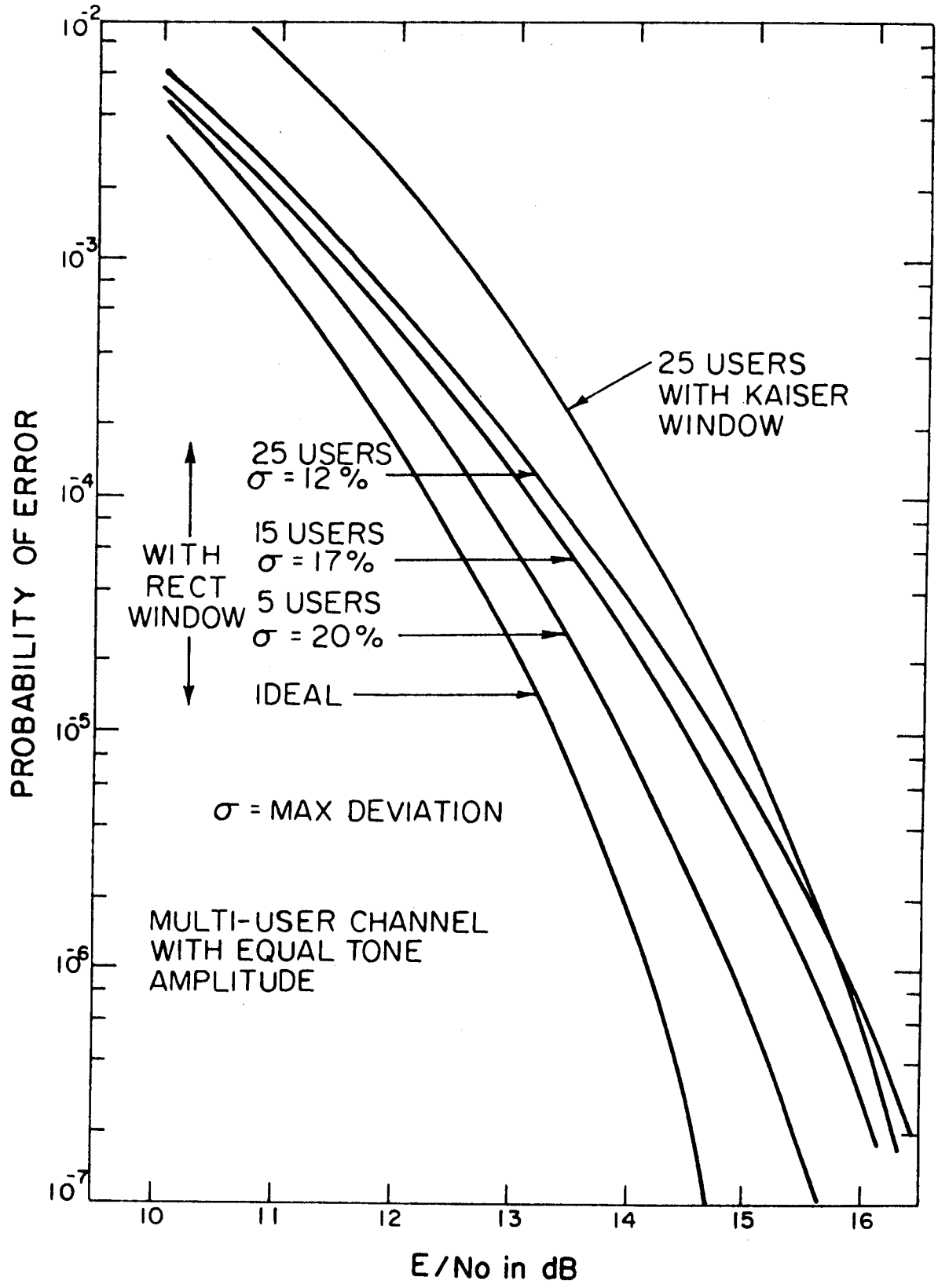

Fig. 8: Average error probability for Binary FSK in a multi-user environment and an AWGN channel. Each user transmits at the same average power.

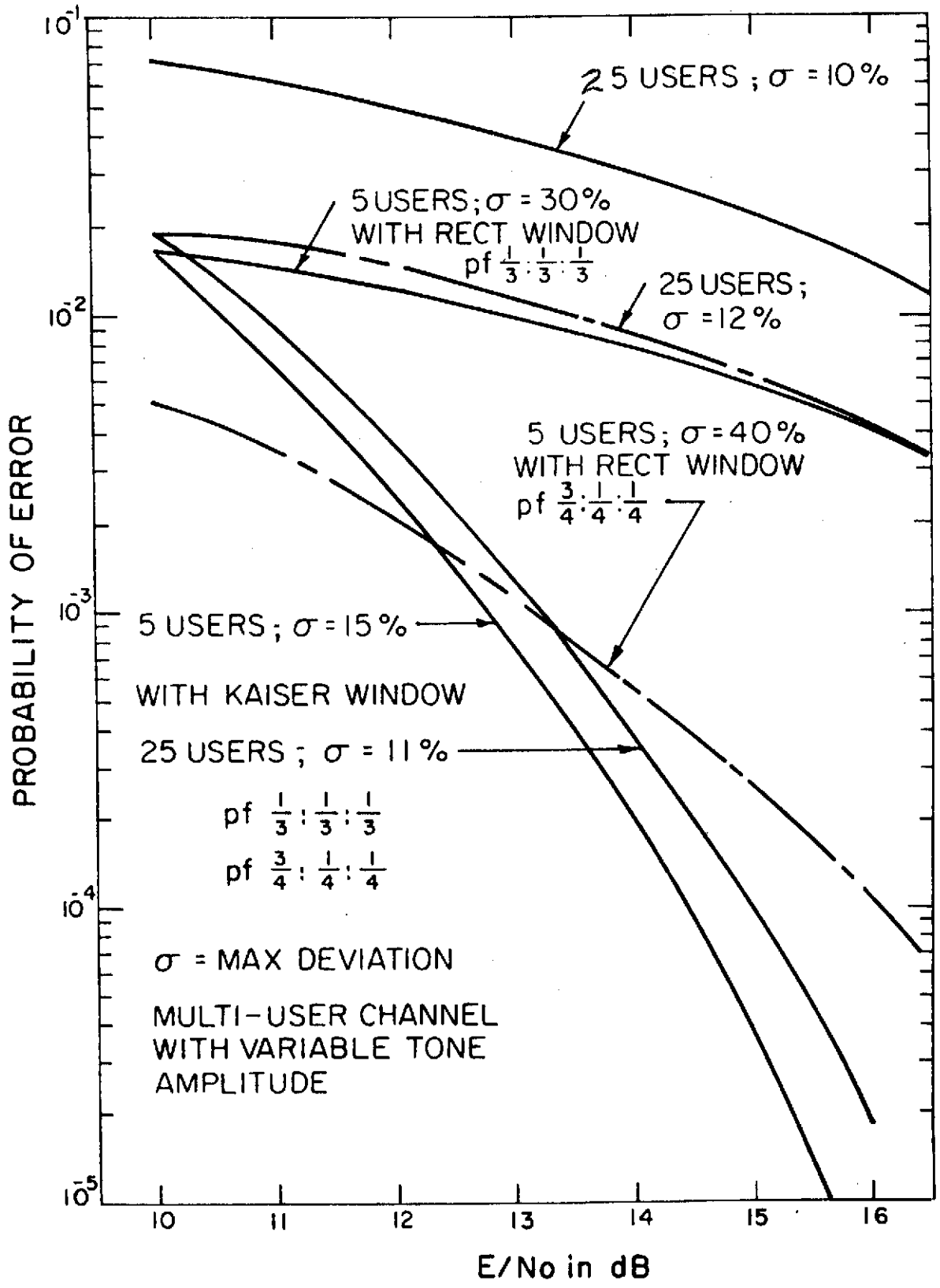

Fig. 9: Average error probability for Binary FSK in a multi-user environment and an AWGN channel. The power levels of the users are randomly changed.

bounds.

Based on Monte Carlo simulations for a 25 user environment it appears that receiver windowing is not required if all users are at the same power level. If a significant variation from equal power occurs then receiver windowing is required.

A random model for computing Binary FSK performance degradation due to frequency errors and a multi-user environment has been presented. We expect this model can be used to handle various jamming scenarios such as partial-band and multi-tone jamming, both in the presence of a loss in system orthogonality in the input signal set.

In the receivers considered, the nominal or unperturbed mark and space frequencies of each user were assumed known at the receiver. We have analyzed receivers in which this is not the case; for instance, a threshold based receiver for declaring tones present or absent. Calculations for such receivers, which are less complex than the ones we have analyzed here, will be available in the coming months. Such a receiver may more closely model the particular receiver implementation described in [13].

REFERENCES

1. G.S. Deshpande and P.H. Wittke, "Correlative encoded digital FM", IEEE Trans. on Communications, vol. COM 29, pp. 156-162, February, 1981.

2. G.S. Deshpande and P.H. Wittke, "Optimum pulse shaping in digital angle modulation", IEEE Trans. on Communications, vol. COM-29, pp. 162-168, February, 1981.

3. P.J. McLane, "The Viterbi receiver for correlative encoded MSK signals", IEEE Trans. Comm., Vol. COM-31, pp. 290-295, Feb. 1983.

4. S.J. Simmons and P.H. Wittke, "Low complexity decoders for constant envelope digital modulations", IEEE Trans. on Communications, accepted for publication.

5. D.J. Vaisey and P.J. McLane, "Realizable Arm filters in I and Q Receivers for MSK-type continuous Phase Modulations", IEEE Globecom, pp. B 7.4.1 - B 7.4.5, Nov. 29 - Dec. 5, 1982, Miami, Florida; accepted for publication, IEEE Trans. on Communications.

6. L.S. Metzger, D.M. Boroson, J.J. Uhran, Jr., and I. Kalet, "Receiver windowing for FDM MFSK signals", IEEE Trans. on Communications, vol. COM 27, pp. 1519-1527, October, 1979.

7. J.J. Spilker, Jr., Digital Communications by Satellite, Prentice-Hall Inc., 1977, p. 378.

8. S.O. Rice, "Mathematical analysis of random noise", Bell Syst. Tech. Jour., Vol. 24, 1945, p. 81.

9. M. Schwartz, W.R. Bennett, and S. Stein, Communication Systems and Techniques McGraw-Hill Inc., 1966, p. 585.

10. W.F. McGee, "Another Recursive Method of Computing the Q-function", IEEE Trans. Info. Theo., Vol. IT-16, pp. 500-501, July 1970.

11. J.M. Wozencraft and I.M. Jacobs, Principles of Communication Engineering, Wiley, New York, 1965.

12. G.D. Forney Jr., "The Viterbi Algorithm", Proc. IEEE, Vol. 61, pp. 268-279, March, 1973.

13. R.R. Rhodes, "Use of Surface Acoustic Wave Reflective Array Compressors in Spectrum Analysis and Demodulation", IEEE EASCON Record, 1979, pp. 283-285.

14. L.E. Franks, Signal Theory, Prentice-Hall Inc., 1969.